

## Accepted Manuscript

Synthesis and characterisation of folic acid based lanthanide ion probes

Zhangli Du, Glenn N. Borlace, Robert D. Brooks, Ross N. Butler, Doug A. Brooks, Sally E. Plush

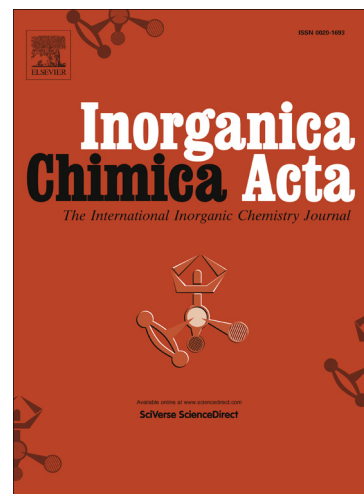
PII: S0020-1693(13)00575-6  
DOI: <http://dx.doi.org/10.1016/j.ica.2013.10.011>  
Reference: ICA 15693

To appear in: *Inorganica Chimica Acta*

Received Date: 23 April 2013  
Revised Date: 9 October 2013  
Accepted Date: 11 October 2013

Please cite this article as: Z. Du, G.N. Borlace, R.D. Brooks, R.N. Butler, D.A. Brooks, S.E. Plush, Synthesis and characterisation of folic acid based lanthanide ion probes, *Inorganica Chimica Acta* (2013), doi: <http://dx.doi.org/10.1016/j.ica.2013.10.011>

This is a PDF file of an unedited manuscript that has been accepted for publication. As a service to our customers we are providing this early version of the manuscript. The manuscript will undergo copyediting, typesetting, and review of the resulting proof before it is published in its final form. Please note that during the production process errors may be discovered which could affect the content, and all legal disclaimers that apply to the journal pertain.



**Synthesis and characterisation of folic acid based lanthanide ion probes**

Zhangli Du<sup>a</sup>, Glenn N Borlace<sup>a</sup>, Robert D Brooks<sup>a</sup>, Ross N Butler<sup>a</sup>, Doug A Brooks<sup>a</sup> and Sally E Plush<sup>a,\*</sup>

<sup>a</sup> *Mechanisms in Cell Biology and Disease Research Group, School of Pharmacy and Medical Sciences, Sansom Institute for Health Research, University of South Australia, 5001, Australia*

*\*Corresponding author: P5-28, Playford building, Frome Rd, Adelaide, SA, 5001, Australia  
Tel: +61 8 830 22586. Fax: +61 8 830 22389. Email: Sally.Plush@unisa.edu.au*

**Abstract:**

As a first step in the process of developing folate based visual probes and contrast agents, we have designed and synthesised a series of first generation lanthanide(III) molecular probes. The molecular probe structure included a lanthanide(III) (Eu(III), Tb(III), Gd(III)) chelate which was linked (**2** or **3**) to either a folic acid or pteronic acid targeting motif. We have defined the emission properties of the molecular probes at different pHs, the emission lifetimes, and the number of metal bound water molecules. The cellular uptake of the molecular probes was investigated in HeLa cells and the amount of Eu(III) internalisation quantified by inductively coupled plasma mass spectrometry. Our results highlighted several key features of probe design: a shorter linker was more optimal for both Eu(III) ion emission intensity and cellular uptake; the folic acid targeting motif exhibited higher cellular uptake when compared to pteronic acid; the emission intensity of the folic acid based probes was pH insensitive, whereas the pteronic acid based probes were pH sensitive. These first generation folate molecular probes displayed promising chemical and physical properties, suggesting that optical and MRI probes can potentially be developed, to enable the imaging of folate receptors in cancer cells and tissues.

**Keywords:**

Lanthanide(III), molecular probe, folic acid, pteronic acid, folate receptor

## 1. Introduction

Molecular probes based on organic fluorophores [1-3], recombinant proteins [4], semiconductor nanoparticles (quantum dots) [5-7] and metal ion complexes [8, 9] have been vital to our understanding of the cellular and molecular mechanisms that occur in different diseases [10-12]. These probes have been used in combination with imaging technologies such as MRI, PET/SPECT, CT and confocal/super resolution microscopy to report on structure and function at the level of individual cells through to whole organisms. There is now a demand for new types of targeted molecular imaging probes that can discriminate between different tissue and cell types. For example, probes that can distinguish between tumour lesions and normal tissue/cells would be of substantial benefit in the detection and treatment of cancer. This kind of specificity can be achieved by using labelled antibodies [13, 14], however there are drawbacks to this approach. For example, the relatively large size of the antibody-conjugate complex compared to the target may affect the behaviour of the target during receptor internalisation/endocytosis. A better approach may be to incorporate targeting motifs directly into the probe structure [15-19]. While there are obvious advantages to this approach with regard to probe specificity and size, the development of molecular imaging probes coupled to specific targeting motifs presents key challenges in design and synthesis. Firstly, the design of the probe should take into account that fluorescence emission can be modulated by pH and or structural changes, and that the signal from the probe can be contaminated by autofluorescence, particularly for live cell imaging applications. Secondly, the synthetic protocols for the probe should ideally be adaptable so that different reporters can be easily incorporated to enable different methods of detection e.g. magnetic resonance vs confocal imaging.

Lanthanide ion complexes have a number of attractive properties that make them suitable candidates for use in both MRI and optical imaging [20-22]. There are a range of commercially available Gd(III) mono-aqua complexes that are routinely used as contrast agents for MRI [23-26]. Other lanthanides (Ln(III) = Sm(III), Eu(III), Tb(III), Dy(III), Yb(III)) are being investigated for use in optical imaging technologies [27-29]. These optically active lanthanides a) possess large Stoke's shifts, which facilitate the easy

separation of excitation from emission wavelengths, b) avoid concentration-dependant self-absorption, which means that the strength of the signal will be proportional to probe concentration, and c) have long emission lifetimes which enables the removal of background autofluorescence in biological samples by using time gated measurements. The lanthanides are also considered to be iso-structural [27], meaning that any single ligand complex combined with any lanthanide ion will retain the same stability and coordination geometry [27, 30]. These qualities provide the capability of generating iso-structural probe sets with a single ligand and a mixed population of lanthanide ions. Thus, administering a “cocktail” of complexes, comprised of a mixture of Gd(III) and Eu(III) ions incorporated with a single ligand, could enable dual detection by MRI and optical imaging. Furthermore, the coupling of a site specific targeting moiety to a lanthanide chelate would enable selective delivery to any cell or tissue with an appropriate receptor. The development of adaptable lanthanide ion based molecular probes with specific targeting motifs may therefore provide a new generation of imaging reagents to visualise disease processes at the molecular level. However, due to the emerging nature of this field, the first priority is to systematically study the effect of structural changes on probe uptake and emission intensity, thereby identifying critical parameters in probe design.

The folate receptor provides an effective model system to evaluate site specific targeting of molecular probes and to investigate the potential of lanthanide molecular probes in biology. This receptor is a cell surface glycosyl-phosphatidylinositol-linked membrane glycoprotein, which has increased expression in several cancers; including colorectal, ovarian, breast, lung, cervical, renal and nasopharyngeal cancers [31-33]. A wide variety of folate receptor targeted systems have already shown promise in cancer biology [18, 34-36]; for example as selective delivery systems for cytotoxic proteins and as real time interoperative fluorescence imaging agents. However, no single system has proven effective both *in vitro* and *in vivo* without concerns over specificity, targeting, side effects or quality of image generated. There are also significant questions regarding the ideal structure of these delivery systems that need to be addressed in terms of; what is the essential binding component of folate and does the glutamic acid residue have a role in folate receptor binding and what is the ideal distance between the folate receptor targeting motif and the imaging agent for example.

Herein, we describe the synthesis and characterisation of a series of first generation folic acid based lanthanide molecular probes [Ln(III) = Eu(III), Tb(III) or Gd(III)]. The basic probe design consisted of a lanthanide chelate coupled to a folate receptor targeting moiety via a linker. A series of probes were synthesised with different linker lengths and different targeting moieties to examine the effect on probe emission and cellular uptake: first, the length of the linker between the folate receptor targeting moiety and the lanthanide chelate was varied, to gain information on the optimal distance for receptor mediated uptake; second, pteric acid (PTE) was substituted for folic acid as the folate receptor targeting moiety. PTE is a sub-component of folic acid (**Figure 1**), which has been shown to target tumour cells with varying efficiency [37, 38]. While synthetic preparations of folic acid are known to produce two regio-isomers, due to the presence of the two carboxylic acid groups in the glutamic acid residue (**Figure 1a**), PTE based probes are synthetically simpler to prepare and still enabled us to examine the efficiency of cellular uptake in response to changes in probe design.

## 2. Experimental

### 2.1. General materials and methods

1,4,7,10-tetraazacyclododecane, Cyclen, was obtained commercially from Strem USA. All other solvents and chemicals used were obtained from Sigma-Aldrich or Merck, Australia. Dowex 1-X8 (Cl) and Sephadex G10 resins were purchased from Sigma-Aldrich, Australia. DO3A<sub>t</sub>Bu (**1**) [39], *N*-(*tert*-butoxycarbonyl)-1,2-diaminoethane [40], *N*-(*tert*-butoxycarbonyl)-1,6-diaminohexane [40, 41], *N*-(2-((2-chloroacetyl)amino)ethyl)-,1,1-dimethylethyl ester (**2**) [30], *N*-(6-((2-chloroacetyl)amino)hexyl)-,1,1-dimethylethyl ester (**3**) were prepared as previously described [30]. Thin layer chromatography (TLC) was performed on silica gel 60 F<sub>254</sub> plates obtained from Merck, Australia. The infrared spectroscopy (IR) was recorded on a Shimadzu FTIR-8400S. Electrospray ionization mass spectrometry (ESI-MS) was recorded using a Perkin-Elmer Sciex API 3000. Inductively coupled plasma mass spectrometry (ICP-MS) was conducted on an Agilent 7500 CS. <sup>1</sup>H NMR and <sup>13</sup>C NMR were recorded on a Bruker 500 MHz NMR spectrometer. All chemical

shifts are given in ppm with coupling constants in Hz. All pH measurements were conducted on an Orion Ross pH meter. Optical spectroscopy experiments were recorded in 100% water at constant ionic strength ( $I = 0.01$  (NaCl)) using a Varian CARY 50 UV-Vis spectrophotometer or a Varian Cary Eclipse spectrophotometer at room temperature. High pressure liquid chromatography (HPLC) was performed on a Shimadzu LC-20AD with manual injection fitted with a Nova-Pak phenyl analytical column (3.9 x 150 mm) with a flow rate of 0.8ml/min and was analysed using a Shimadzu SPD-20A detector at 280 nm. Isocratic elution was used with the mobile phases 70% A (H<sub>2</sub>O+0.1% TFA) and 30% B (CH<sub>3</sub>OH+0.1% TFA). The ICP-MS was performed at the University of Adelaide; CNH analysis was conducted in Campbell Microanalytical Laboratory, University of Otago.

## 2.2. Synthesis

### 2.2.1. 1,4,7-Tris(*tert*-butoxycarbonylmethyl)-10-(*N*-(2-*tert*-butoxycarbonylaminoethyl)acetamide)-1,4,7,10-tetraazacyclododecane (**4**)

A solution of **1** (294 mg, 0.57 mmol), **2** (139 mg, 0.59 mmol) and Cs<sub>2</sub>CO<sub>3</sub> (326 mg, 1.2 mmol) were stirred in CH<sub>3</sub>CN (20 ml) at 65 °C for 24 h. The reaction mixture was filtered through celite and the solvent was removed under reduced pressure. DCM (30 ml) was added to the residue and the organic layers washed with water (3 x 20 ml), dried over Na<sub>2</sub>SO<sub>4</sub> and the solvent removed under reduced pressure to yield the product as a yellow oil. Yield: 380 mg (93%). IR (KBr)  $\nu = 3341$  (br), 2978, 2936, 2870, 2828, 1728, 1670, 1524, 1454, 1431, 1370, 1250, 1227, 1161, 1103, 1007 cm<sup>-1</sup>. <sup>1</sup>H NMR (CDCl<sub>3</sub>, 500 MHz) (Fig. S1 in the supplementary materials):  $\delta$  3.36 to 3.25 (br m, approx. 16H (not resolved), CH<sub>2</sub>), 2.89 to 2.50 (br m, approx. 12H (not resolved), CH<sub>2</sub>), 1.45 (t, approx. 36H (not resolved), CH<sub>3</sub>); <sup>13</sup>C NMR (CDCl<sub>3</sub>, 125.8 MHz):  $\delta$  172.2 (C=O), 170.3 (C=O), 156.6 (C=O), 156.1 (C=O), 82.0 (C), 81.4 (C), 79.0 (C), 56.4 (CH<sub>2</sub>), 56.0 (CH<sub>2</sub>), 55.7 (CH<sub>2</sub>), 52.5 (CH<sub>2</sub>), 40.9 (CH<sub>2</sub>), 40.1 (CH<sub>2</sub>), 39.8 (CH<sub>2</sub>), 30.9 (CH<sub>2</sub>), 28.5 (CH<sub>2</sub>), 28.2 (br, CH<sub>3</sub>). ESI-MS<sup>+</sup>:  $m/z = 715.7$  (M+1)<sup>+</sup>, (99); 659.4 (100); 603.6 (99).

### 2.2.2. 1,4,7-Tris(*tert*-butoxycarbonylmethyl)-10-(*N*-(2-*tert*-butoxycarbonylaminoethyl)acetamide)-1,4,7,10-tetraazacyclododecane (**5**)

Compound **5** was prepared as described for **4** except that **3** (259 mg, 0.88 mol) was reacted with **1** (463 mg, 0.90 mol) and Cs<sub>2</sub>CO<sub>3</sub> (69 mg, 0.21 mmol) instead of **2**. The product was obtained as a yellow oil. Yield: 560 mg (98%). IR (KBr)  $\nu$  = 3383 (br), 2978, 2932, 2855, 2824, 1728, 1663, 1524, 1458, 1370, 1308, 1250, 1227, 1161, 1107 cm<sup>-1</sup>. <sup>1</sup>H NMR (CDCl<sub>3</sub>, 500 MHz) (Fig. S2 in the supplementary materials):  $\delta$  3.12 (m, 8H, CH<sub>2</sub>), 3.06 (br, 4H, CH<sub>2</sub>), 2.79 (m, 16H, ) 1.41-1.29 (br m, approx. 44H (not resolved), CH<sub>2</sub> and CH<sub>3</sub>); <sup>13</sup>C NMR (CDCl<sub>3</sub>, 125.8 MHz):  $\delta$  172.3 (C=O), 171.5 (C=O), 170.6 (C=O), 156.0 (C=O), 81.8 (C(CH<sub>3</sub>)<sub>3</sub>), 81.1 (C(CH<sub>3</sub>)<sub>3</sub>), 78.9 (C(CH<sub>3</sub>)<sub>3</sub>), 56.6 (br, CH<sub>2</sub>), 56.2 (CH<sub>2</sub>), 52.6 (CH<sub>2</sub>), 42.7 (br, CH<sub>2</sub>), 40.5 (CH<sub>2</sub>), 40.0 (CH<sub>2</sub>), 39.2 (CH<sub>2</sub>), 30.0 (br, CH<sub>2</sub>), 28.4 (CH<sub>3</sub>), 28.2 (CH<sub>3</sub>), 26.7 (br, CH<sub>2</sub>). ESI-MS<sup>+</sup>:  $m/z$  = 771.8 (M+1)<sup>+</sup>, (40); 715.8 (100); 659.8 (15); 615.8 (70).

#### 2.2.3. 1,4,7-Tris(carbonylmethyl)-10-(aminoethyl-*N'*-acetyl)-1,4,7,10-tetraazacyclododecane (**6**)

Compound **4** (360 mg, 0.50 mmol) was dissolved in a DCM/TFA (1/1) solution and stirred at room temperature overnight. The solvent was then removed under reduced pressure to yield a brown residue. The residue was then re-dissolved in water and the pH of the solution adjusted to pH 7 using 1 M NaOH. The solvent was removed under reduced pressure to yield the product as a hygroscopic solid in quantitative yield. This was used in the next step without further purification. IR (KBr)  $\nu$  = 3449 (br), 1686, 1640, 1435, 1404, 1207, 1134 cm<sup>-1</sup>. <sup>1</sup>H NMR (D<sub>2</sub>O, 500 MHz) (Fig. S3 in the supplementary materials):  $\delta$  3.84 (m, 4H, CH<sub>2</sub>), 3.64 (br, 2H, CH<sub>2</sub>), 3.54 – 3.42 (m, 10H, CH<sub>2</sub>), 3.35 (s, 2H, CH<sub>2</sub>), 3.21 (m, 2H, CH<sub>2</sub>), 3.13 (br, 4H, CH<sub>2</sub>), 2.95 (br, 2H, CONHCH<sub>2</sub>), 2.88 (br, 2H, NH<sub>2</sub>CH<sub>2</sub>); <sup>13</sup>C NMR (CDCl<sub>3</sub>, 125.8 MHz) (Fig. S4 in the supplementary materials):  $\delta$  178.9 (C=O), 173.2 (C=O), 170.1 (C=O), 57.3 (CH<sub>2</sub>), 56.3 (CH<sub>2</sub>), 56.2 (CH<sub>2</sub>), 52.1 (CH<sub>2</sub>), 50.4 (CH<sub>2</sub>), 48.8 (CH<sub>2</sub>), 48.4 (CH<sub>2</sub>), 39.1 (CH<sub>2</sub>), 36.8 (CH<sub>2</sub>). ESI-MS<sup>+</sup>:  $m/z$  = 447.5 (M+1)<sup>+</sup>.

#### 2.2.4. 1,4,7-Tris(carbonylmethyl)-10-(aminohexyl-*N'*-acetyl)-1,4,7,10-tetraazacyclododecane (**7**)

Compound **7** was prepared using the same methodology as described for **6** except that **5** (580 mg, 0.75 mmol) was used instead of **4**. The product was obtained as a hygroscopic solid

quantitatively and used for next step without further purification. IR (KBr)  $\nu = 3449$  (br), 3094 (br), 2947, 2870, 1732, 1674, 1462, 1427, 1389, 1354, 1316, 1200, 1022 (br)  $\text{cm}^{-1}$ .  $^1\text{H}$  NMR ( $\text{D}_2\text{O}$ , 500 MHz) (Fig. S5 in the supplementary materials):  $\delta$  3.73 (m, 8H,  $\text{CH}_2$ ), 3.40 (m, 10H,  $\text{CH}_2$ ), 3.02 (m, 10H,  $\text{CH}_2$ ), 1.59 (m, 2H,  $\text{CH}_2\text{CH}_2\text{CH}_2$ ), 1.46 (m, 2H,  $\text{CH}_2\text{CH}_2\text{CH}_2$ ), 1.30 (m, 4H,  $\text{CH}_2\text{CH}_2\text{CH}_2$ );  $^{13}\text{C}$  NMR ( $\text{CDCl}_3$ , 125.8 MHz) (Fig. S6 in the supplementary materials):  $\delta$  178.2 (C=O), 171.8 (C=O), 170.0 (C=O), 56.6 ( $\text{CH}_2$ ), 56.2 ( $\text{CH}_2$ ), 55.9 ( $\text{CH}_2$ ), 51.8 ( $\text{CH}_2$ ), 50.9 ( $\text{CH}_2$ ), 48.3 ( $\text{CH}_2$ ), 39.4 ( $\text{CH}_2$ ), 39.1 ( $\text{CH}_2$ ), 28.0 ( $\text{CH}_2$ ), 26.5 (d,  $\text{CH}_2$ ), 25.4 ( $\text{CH}_2$ ), 25.0 ( $\text{CH}_2$ ). ESI-MS<sup>+</sup>:  $m/z = 503.7$  (M+1)<sup>+</sup>.

#### 2.2.5. 1,4,7-Tris(carbonylmethyl)-10-(aminoethyl-*N'*-acetyl)-1,4,7,10-tetraazacyclododecane.Eu (**6**.Eu, **8**)

Compound **6** (484 mg, 1.1 mmol) and  $\text{Eu}(\text{CF}_3\text{SO}_3)_3$  (649 mg, 1.1 mmol) were dissolved in  $\text{CH}_3\text{OH}$  (8 ml) and stirred at 65 °C for 24 h under  $\text{N}_2$ . The solvent was then removed under reduced pressure. The unreacted  $\text{Eu}(\text{CF}_3\text{SO}_3)_3$  and any excess salt from the previous step were removed by a Sephadex G10 column in  $\text{CH}_3\text{OH}$  to yield the product as a yellow powder. Yield: 300 mg (47%). IR (KBr)  $\nu = 3426$  (br), 2994, 2924, 2878, 1586, 1443, 1408, 1273, 1254, 1173, 1084, 1030  $\text{cm}^{-1}$ . Calculated for  $\text{C}_{18}\text{H}_{34}\text{EuN}_6\text{O}_7^{3+} \cdot 3\text{CF}_3\text{SO}_3^{3-} \cdot 2\text{H}_2\text{O}$ : C, 23.32; H, 3.54; N, 7.77. Found: C, 23.20; H, 3.76; N, 7.57. For elemental analysis complex **8** was dissolved in water ( $\text{H}_2\text{O}$ ) and freeze dried.  $^1\text{H}$  NMR ( $\text{D}_2\text{O}$ , 500 MHz) (Fig. S7 in the supplementary materials):  $\delta$  33.68, 31.61, 30.48, 12.15, 11.03, 10.42, 7.07, 5.95, 4.91 to 1.40 (m), 0.48, -0.47, -2.22, -2.45, -3.32, -4.97, -5.49, -7.40, -7.73, -8.03, -10.99, -11.39, 12.55, -13.66, -14.00, -14.86, -15.64, -16.74. ESI-MS<sup>+</sup>:  $m/z = 597.4$  (M+1)<sup>+</sup>. HPLC: method A,  $t = 2.2$  min (Fig. S15 in the supplementary materials).

#### 2.2.6. 1,4,7-Tris(carbonylmethyl)-10-(aminoethyl-*N'*-acetyl)-1,4,7,10-tetraazacyclododecane.Tb (**6**.Tb, **9**)

The lanthanide complex, **9** was prepared in a similar manner as described for complex **8**; **6** (135 mg, 0.30 mmol) was reacted with  $\text{Tb}(\text{CF}_3\text{SO}_3)_3$  (185 mg, 0.31 mmol) in  $\text{CH}_3\text{OH}$ . Complex **9** was obtained as a yellow powder. Yield: 76 mg (41%). IR (KBr)  $\nu = 3487$  (br), 1609, 1261, 1234, 1173, 1038  $\text{cm}^{-1}$ .  $^1\text{H}$  NMR ( $\text{D}_2\text{O}$ , 500 MHz) (Fig. S8a – S8b in the

supplementary materials):  $\delta$  252.38, 242.72, 204.38, 196.23, 120.76, 111.40, 73.06, 50 to -50 (br), -62.59, -75.11, -82.23, -96.22, -109.23, -118.56, -134.03, -364.03, -376.05, -378.51, -406.98. ESI-MS<sup>+</sup>:  $m/z$  = 603.2 (M+1)<sup>+</sup>.

2.2.7. 1,4,7-Tris(carbonylmethyl)-10-(aminoethyl-*N'*-acetyl)-1,4,7,10-tetraazacyclododecane.Gd (**6.Gd,10**)

The lanthanide complex, **10** was prepared in a similar manner as described for complex **8**; **6** (43 mg, 0.097 mmol) was reacted with Gd(CF<sub>3</sub>SO<sub>3</sub>)<sub>3</sub> (62 mg, 0.10 mmol) to obtain **10** as a yellow powder. Yield: 45 mg (77 %). IR (KBr)  $\nu$  = 3433 (br), 1686, 1609, 1451, 1412, 1261, 1196, 1173, 1084, 1038 cm<sup>-1</sup>. ESI-MS<sup>+</sup>:  $m/z$  602.2 (M+1)<sup>+</sup>.

2.2.8. 1,4,7-Tris(carbonylmethyl)-10-(aminohexyl-*N'*-acetyl)-1,4,7,10-tetraazacyclododecane.Eu (**7.Eu, 11**)

The lanthanide complex, **11** was prepared in a similar manner as described for complex **8**, except that **7** (368 mg, 0.73 mmol) was reacted with Eu(CF<sub>3</sub>SO<sub>3</sub>)<sub>3</sub> (461 mg, 0.77 mmol) in CH<sub>3</sub>OH instead of **6**. Complex **11** was obtained as a yellow powder. Yield: 246 mg (52%). IR (KBr)  $\nu$  = 3426 (br), 3109, 2940, 2870, 1620, 1439, 1400, 1323, 1277, 1250, 1204, 1169, 1084, 1030, 1003 cm<sup>-1</sup>. Calculated for C<sub>22</sub>H<sub>41</sub>EuN<sub>6</sub>O<sub>7</sub><sup>2+</sup>.2CF<sub>3</sub>SO<sub>3</sub><sup>2-</sup>.2CH<sub>3</sub>OH.COHN(CH<sub>3</sub>)<sub>2</sub>: C, 31.99; H, 5.18; N, 9.00. Found: C, 32.13; H, 4.96; N, 8.99. For elemental analysis complex **11** was dissolved in dimethylformamide (COHN(CH<sub>3</sub>)<sub>2</sub>) and freeze dried. <sup>1</sup>H NMR (D<sub>2</sub>O, 500 MHz) (Fig. S9 in the supplementary materials):  $\delta$  33.16, 32.80, 31.90, 31.66, 12.88 (d), 12.18 (d), 4.09 to 1.12 (m), 0.70, 0.39, -0.09, -0.30, -0.50, -1.69, -2.61, -4.25, -5.24, -6.00, -6.54, -7.20, -7.79, -9.87, -10.79, -12.66, -12.91, -15.10, -15.30, -16.03. ESMS<sup>+</sup>:  $m/z$  653.3 (M+1)<sup>+</sup>. HPLC:  $t$  = 2.7 min (Fig. S16 in the supplementary materials).

2.2.9. 1,4,7-Tris(carbonylmethyl)-10-(aminohexyl-*N'*-acetyl)-1,4,7,10-tetraazacyclododecane.Gd (**7.Gd, 12**)

The lanthanide complex, **12** was prepared in a similar manner as described for complex **8**, except that **7** (48 mg, 0.095mmol) was reacted with Gd(CF<sub>3</sub>SO<sub>3</sub>)<sub>3</sub> (61 mg, 0.10 mmol) in

CH<sub>3</sub>OH instead of **6**. **12** was obtained as a yellow powder. Yield: 51 mg (82%). IR (KBr)  $\nu$  = 3422 (br), 2943, 2859, 1678, 1636, 1605, 1454, 1397, 1254, 1204, 1173, 1084, 1038 cm<sup>-1</sup>. ESI-MS<sup>+</sup>:  $m/z$  657.8 (M+1)<sup>+</sup>.

#### 2.2.10. [6.Eu]-pteroic acid (**13**)

Pterioic acid (50 mg, 0.16 mmol) was dissolved in DMSO (2ml) by the assistance of sonication, after which *N,N*-Diisopropylethylamine (DIPEA) (42 mg, 0.32 mmol) was added. The reaction mixture was stirred for 10 min, then 1-Hydroxybenzotriazole (HOBt) (23 mg, 0.17 mmol) and (Benzotriazol-1-yloxy) tris (dimethylamino) phosphonium hexafluorophosphate (BOP) (74 mg, 0.17 mmol) were added and the reaction mixture was stirred for a further 2 hours. Following this, a solution of **8** (96 mg, 0.16 mmol) and DIPEA (21 mg, 0.16 mmol) in DMSO (1 ml) was added. The reaction mixture was left to stir at room temperature, protected from the light, overnight. The crude product was precipitated out by adding 10 ml of diethyl ether/acetone (7/3) and collected by centrifugation.

The crude product was dissolved in a minimal amount of NaOH (pH 10), and carefully loaded onto a Dowex 1-X8 column (CI). Water was used to elute the product and fractions were collected and analysed by MS and TLC. Fractions containing the product were combined and the pH adjusted to pH 7. The solvent was then removed under reduced pressure to yield a yellow residue. In order to extract the product from excess salt, DMSO (1 ml) was added to the residue, the solution was then centrifuged and the supernatant collected. The product was then isolated from the DMSO solution through precipitation following the addition of diethyl ether/acetone (7/3). The product was dried and washed by CH<sub>3</sub>OH. The solvent residue was removed under reduced pressure and the product was further dried by vacuum to yield **13** as a yellow powder. Yield: 38 mg (21%). TLC: silica isopropanol/ammonia (5 M) (7/3), R<sub>f</sub> 0.2. IR (KBr)  $\nu$  = 3433 (br), 2920, 2866, 1609, 1512, 1400, 1323, 1242, 1180, 1130, 1084 cm<sup>-1</sup>. <sup>1</sup>H NMR (D<sub>2</sub>O, 500 MHz) (Fig. S10 in the supplementary materials):  $\delta$  34.00, 32.81, 31.35 (br), 30.66, 13.14, 12.10, 11.53, 10.91, 9.30 to 1.61 (m), 0.62, 0.38, -0.73 (br), -1.73 (br), -2.54 (br), -3.19, -3.77, -5.46, -5.88, -7.11 (d), -7.53, -7.95 (br), -8.68, -9.84, -10.99 (br), -11.64 (br), -12.02, -12.60, -14.56, -14.79, -15.37, -

15.60, -16.21, -17.02, -17.48. ESI-MS<sup>+</sup>:  $m/z = 891.4 (M+1)^+$ . HPLC: method A,  $t = 4.9$  min (Fig. S17 in the supplementary materials).

#### 2.2.11. [7.Eu]-pteroic acid (**14**)

The Eu(III) complex, **14**, was prepared and purified in a similar manner as described for Eu(III) complex **13**; Pteric acid (75 mg, 0.24 mmol), BOP (119 mg, 0.27 mmol), HOBT (33 mg, 0.25 mmol), DIPEA (93 mg, 0.72 mmol) and **11** (157 mg, 0.24 mmol) in DMSO (3 ml) and purified by Dowex 1-X8 (Cl) column to yield a yellow powder. Yield: 42 mg (22%). TLC: silica isopropanol/ammonia (5 M) (7/3),  $R_f$  0.3. IR (KBr)  $\nu = 3437$  (br), 2920, 2866, 1613, 1512, 1389, 1261, 1173, 1134, 1084, 1034  $\text{cm}^{-1}$ . <sup>1</sup>H NMR (D<sub>2</sub>O, 500 MHz) (Fig. S11 in the supplementary materials):  $\delta$  32.21, 32.69, 31.78, 12.50 (br), 8.47 to 1.07 (m), -0.09, -0.39, -1.73, -2.74, -4.13, -5.18, -6.03, -6.67, -7.28, -7.82 (br), -10.09 (br), -10.77 (br), -12.56, -12.87, -15.27, -16.15. ESI-MS<sup>+</sup>:  $m/z = 947.5 (M+1)^+$ . HPLC: method A,  $t = 13.7$  min (Fig. S18 in the supplementary materials).

#### 2.2.12. [6.Eu]-folic acid (**15**)

The Eu(III) complex, **15**, was prepared and purified in a similar manner as described for Eu(III) complex **13**; by using folic acid (74 mg, 0.17 mmol), BOP (76 mg, 0.17 mmol), HOBT (23 mg, 0.17 mmol), DIPEA (65 mg, 0.50 mmol) and **8** (101 mg, 0.17 mmol) in DMSO (3 ml) to yield the crude product. However, the following purification was used instead: The crude product was dissolved in a minimal amount of 20 mM sodium phosphate buffer (pH 10), and carefully loaded onto a Sephadex G10 column that had been pre-equilibrated by the same buffer system overnight. The fractions were collected, checked by TLC and altered to pH 7, then dried under reduced pressure. DMSO was added to extract the product from salt, the solution centrifuged, the supernatant collected and the product precipitated out by the addition of diethyl ether /acetone (7/3). The product was dried and washed by CH<sub>3</sub>OH. The solvent was removed under reduced pressure and the product further dried by vacuum line to yield a yellow powder. Yield: 73 mg (43%). TLC: silica isopropanol/ammonia (5 M) (7/3),  $R_f$  0.2. IR (KBr)  $\nu = 3383$  (br), 2920, 2866, 2805, 1728, 1690, 1605, 1512, 1409, 1319, 1296, 1177, 1130, 1084, 1018  $\text{cm}^{-1}$ . <sup>1</sup>H NMR (D<sub>2</sub>O, 300 MHz) (Fig. S12 in the supplementary materials):  $\delta$  33.55, 33.10, 31.48, 30.64, 12.05 (br), 11.41 (br), 8.66 to 1.26

(m), -0.04, -0.56, -2.31, -3.27, -5.00, -5.64, -7.27, -7.54, -10.76, -11.29, -11.67, -11.95, -12.63, -13.97, -14.26, -14.95, -15.49, -16.58. ESI-MS<sup>+</sup>:  $m/z = 1020.7 (M+1)^+$ . HPLC: method A,  $t = 4.8$  min, 5.6 min (Fig. S19 in the supplementary materials).

#### 2.2.13. [7.Eu]-folic acid (**16**)

The Eu(III) complex, **16** was synthesised and purified as describe for complex **15** except that Eu(III) complex **11** (101 mg, 0.16 mmol) was used instead of the Eu(III) complex **8** with folic acid (70 mg, 0.15 mmol), BOP (68 mg, 0.15 mmol), HOBt (21 mg, 0.15 mmol), DIPEA (59 mg, 0.46 mmol) in DMSO (3 ml) and purified with a Sephadex G10 column to yield the product. Yield: 66 mg (40%). TLC: silica isopropanol/ammonia (5 M) (7/3),  $R_f$  0.3. IR (KBr)  $\nu = 3433$  (br), 2932, 2862, 1616, 1508, 1400, 1323, 1242, 1204, 1180, 1130, 1084, 1018  $\text{cm}^{-1}$ . <sup>1</sup>H NMR (D<sub>2</sub>O, 500 MHz) (Fig. S13 in the supplementary materials):  $\delta$  33.00 (d), 31.81 (d), 12.91 (br), 12.11 (br), 9.06 to 0.89 (m), 0.44, -0.07, -0.29, -0.48, -1.72, -2.64, -4.26 (br), -5.17, -5.98, -6.49 (br), -7.19, -7.78 (br), -9.80 (br), -10.75 (br), -12.62 (br), -12.84, -15.15, -16.07. ESI-MS<sup>+</sup>:  $m/z = 1076.7 (M+1)^+$ . HPLC: method A,  $t = 14.3$  min, 19.6 min (Fig. S20 in the supplementary materials).

#### 2.2.14. [6.Tb]-pteroic acid (**17**)

The Tb(III) complex, **17**, was prepared and purified in a similar manner as described for Eu(III) complex **13**; Pterioic acid (13 mg, 0.042 mmol), BOP (20 mg, 0.045 mmol), HOBt (6 mg, 0.047 mmol), DIPEA (16 mg, 0.13 mmol) and **9** (25 mg, 0.042 mmol) in DMSO (3 ml) and purified by Dowex 1-X8 (CI) column to yield a yellow powder. Yield: 12 mg (32%). TLC: silica isopropanol/ammonia (5 M) (7/3),  $R_f$  0.4. IR (KBr)  $\nu = 3426$  (br), 2924, 2874, 1605, 1512, 1400, 1319, 1285, 1242, 1188, 1161, 1119, 1084, 1003  $\text{cm}^{-1}$ . <sup>1</sup>H NMR (D<sub>2</sub>O, 500MH) (Fig. S14a – S14b in the supplementary materials):  $\delta$  257.43, 242.17, 202.83, 193.15, 111.25, 104.79, 50 to -50 (br), -68.41, -76.42, -79.51, -101.39, -110.32, -116.18, -125.11, -369.18, -378.42, -381.81, -398.15. ESI-MS<sup>+</sup>:  $m/z = 897.8 (M+1)^+$ . HPLC: method A,  $t = 5.1$  min (Fig. S21 in the supplementary materials).

2.2.15. [6.Gd]-pteroic acid (**18**)

The Gd(III) complex, **18**, was prepared and purified in a similar manner as described for Eu(III) complex **13**; Pteric acid (24 mg, 0.077 mmol), BOP (35 mg, 0.079 mmol), HOBT (10 mg, 0.077 mmol), DIPEA (29.1 mg, 0.23 mmol) and **10** (45 mg, 0.075 mmol) in DMSO (3 ml) and purified by Dowex 1-X8 (CI) column to yield a yellow powder. Yield: 30.5 mg (44%). TLC: silica isopropanol/ammonia (5M) (7/3), R<sub>f</sub> 0.3. IR (KBr)  $\nu = 3418$  (br), 2924, 2870, 1605, 1508, 1439, 1404, 1319, 1242, 1192, 1161, 1123, 1084, 1003 cm<sup>-1</sup>. ESI-MS<sup>+</sup>:  $m/z$  896.3 (M+1)<sup>+</sup>. HPLC:  $t = 5.0$  min (Fig. S22 in the supplementary materials).

2.2.16. [7.Gd]-pteroic acid (**19**)

The Gd(III) complex, **19**, was prepared and purified in a similar manner as described for Eu(III) complex **13**; Pteric acid (17.4 mg, 0.056 mmol), BOP (26.4 mg, 0.060 mmol), HOBT (9.2 mg, 0.068 mmol), DIPEA (22 mg, 0.17 mmol) and **12** (36.9 mg, 0.056 mmol) in DMSO (3 ml) and purified by Dowex 1-X8 (CI) column to yield a yellow powder. Yield: 19 mg (36%). TLC: silica isopropanol/ammonia (5M) (7/3), R<sub>f</sub> 0.3. IR (KBr)  $\nu = 3426$  (br), 2924, 2862, 1609, 1404, 1389, 1319, 1246, 1180, 1084, 1018 cm<sup>-1</sup>. ESI-MS<sup>+</sup>:  $m/z$  952.6 (M+1)<sup>+</sup>. HPLC:  $t = 12.3$  min (Fig. S23 in the supplementary materials).

2.2.17. [6.Gd]-folic acid (**20**)

The Gd(III) complex, **20** was synthesised and purified as describe for the Eu(III) complex, **15** except that the Gd(III) complex **10** (40 mg, 0.067 mmol) was used instead of the Eu(III) complex, **8** with folic acid (29 mg, 0.067 mmol), BOP (30 mg, 0.068 mmol), HOBT (11 mg, 0.081 mmol), DIPEA (27 mg, 0.21 mmol) in DMSO (3 ml) and purified with a Sephadex G10 column to yield the product. Yield: 24 mg (35%). TLC: silica isopropanol/ammonia (5M) (7/3), R<sub>f</sub> 0.3. IR (KBr)  $\nu = 3403$  (br), 3106 (br), 2893 (br), 1597, 1501, 1400, 1335, 1126, 1042. ESI-MS<sup>+</sup>:  $m/z$  1025.7 (M+1)<sup>+</sup>. HPLC:  $t = 5.0$  min, 5.7 min (Fig. S24 in the supplementary materials).

### 2.3. Cellular uptake

HeLa cells (human endothelial carcinoma cell line, ATCC CCL-2), were cultured in DMEM/F-12 (Dulbecco's Modified Eagle Medium/F-12, Gibco, Life Technologies, USA) supplemented with 10% Foetal Bovine Serum (In Vitro Technologies, Vic, Australia), in a 5% CO<sub>2</sub> atmosphere at 37 °C. Cells were cultured to ~80% confluence in T-75 flasks (In Vitro Technologies) before overnight (16 hours) incubation with Eu(III) probes (**13**, **14**, **15** and **16**) dissolved in fresh cell culture medium. Cells were washed 3 times in Dulbecco's phosphate buffered saline (DPBS, SAFC Biosciences, USA) and detached from the flask by treatment with TrypLE Express (Gibco, Life Technologies, USA) for 10 min at 37 °C before being pelleted (400xg, 5 min) and resuspended in 5 ml DPBS. A 0.5 ml aliquot was taken for trypan blue exclusion cell counts and protein determination by the bicinchoninic acid (BCA) protein assay. The protein assay aliquots were centrifuged (16,000xg, 3 min) and the pellets resuspended in 35 µl lysis buffer (10 mM Tris pH 7.5, 100 mM NaCl, 1mM EDTA, 1% (v/v) TritonX-100) containing protease inhibitors (Complete Mini EDTA-free Protease Inhibitor Cocktail Tablets, Roche, USA) and incubated overnight (16 hours) at 4 °C. Total protein content was determined using the Micro BCA protein Assay kit according to the manufacturer's instructions (Thermo Scientific, USA). The remaining cells (4.5 ml) were centrifuged (400xg, 5 min) and the pellet was resuspended in 5 ml 5% HNO<sub>3</sub>. After 3 days the acid treated cells were filter sterilised through a 0.22 µm syringe filter (Millipore, Ireland) and the supernatant analysed by inductively coupled plasma mass spectrometry (ICP-MS) to determine the Eu(III) concentration in parts per billion; using an Agilent 7500CS (Adelaide Microscopy, University of Adelaide). The Eu(III) counts were normalised to the amount of cellular protein (nmol Eu/mg of protein). Haemocytometer cell counts determined that 1 mg of protein corresponded to 2.5 x 10<sup>6</sup> cells; and the final intracellular concentration of Eu(III) was calculated using an assumed individual cell volume of 5000 µm<sup>3</sup> [42].

## 3. Results and Discussion

### 3.1. Synthesis of the complexes

The synthetic pathway outlined in **Scheme 1** describes the synthesis of the folate receptor targeted lanthanide complexes **13-20** from the tri-Boc protected cyclen precursor (DO3A/Bu)

(1). This pathway was designed to be easily adapted to different targeting moieties, in this work the two folate receptor targeting moieties, PTE and folic acid, were used. However, it is anticipated that this pathway could be further adapted to any targeting moiety with a reactive carboxylate functionality. Furthermore, it was designed to allow the facile introduction of different Ln(III) ions to generate a series of isostructural Ln(III) ion complexes.

The Boc protected chloroacetamide linker derivatives **2** and **3** were prepared as described by Fanning and co-workers [30]. Mono protection of both ethylene and hexane diamine was achieved by the addition of di-*tert*-butyl dicarbonate at 0 °C; which was then reacted with chloroacetyl chloride in the presence of triethylamine in DCM at 0 °C to yield the  $\alpha$ -chloroacetamide derivatives **2** and **3** in 62% and 54% yield, respectively. The tetra substituted ligands **4** and **5** were formed by the reaction of (DO3A*t*Bu) with **2** and **3**, in dry CH<sub>3</sub>CN in the presence of Cs<sub>2</sub>CO<sub>3</sub> at 65 °C for 24 hours. This generated **4** and **5**, respectively, in high yield. The deprotection of both the *t*-butyl and carbamate esters was achieved using a 1/1 ratio of trifluoroacetic acid in DCM, generating the ligands **6** and **7** as hygroscopic solids. The Ln(III) complexes (**8-12**), were prepared by refluxing each of the ligands with 1 to 1.1 molar equivalents of the relevant lanthanide triflate in dry CH<sub>3</sub>OH under nitrogen for 24 hours. The lanthanide complexes were then purified using a sephadex G10 column to ensure complete removal of excess salt and lanthanide ions, isolating the lanthanide complexes **8-12** as yellow powders.

The <sup>1</sup>H NMR spectra of the Eu(III) complexes (**8** and **11**) in D<sub>2</sub>O showed resonances between +34 ppm and -17 ppm, with peaks around +34 to +30 ppm and +14 to +10 ppm, which were characteristic of square antiprismatic geometry and twisted square antiprismatic geometry (Fig. S7 and S9 in the supplementary materials). This was consistent with other cyclen complexes in solution [43, 44]. The Eu(III) complexes (**8** and **11**), were fully characterised by elemental analysis, HPLC, IR, ESI-MS and NMR spectroscopy. These Eu(III) complexes were then reacted with either folic acid or PTE using the amide coupling reagents, 1-Hydroxybenzotriazole (HOBt) and (Benzotriazol-1-yloxy) tris (dimethylamino) phosphonium hexafluorophosphate (BOP) in the presence of *N,N*-diisopropylethylamine (DIPEA) in DMSO. The PTE based Eu(III) probes, **13** and **14**, were purified using an ion exchange

column loaded with Dowex 1-X8 (Cl); probes were obtained with a 20-40% yield. As folic acid has two carboxylic acid groups at the  $\alpha$  and  $\gamma$  positions, the coupling of the Eu(III) complexes **8** and **11** with folic acid can produce both the expected regio-isomers and a bis-coupled product. There was, however, no evidence for the formation of the bis-coupled product in the mass spectra of either the reaction mixtures or the purified products, which was attributed to steric hindrance. Purification of the folic acid based Eu(III) based probes (**15** and **16**) was achieved using a sephadex G10 column with 20 mM phosphate buffer at pH 10. The  $^1\text{H}$  NMR spectra of the folic acid and PTE based Eu(III) probes (**13-16**) in  $\text{D}_2\text{O}$  were consistent with the molecular probes adopting square antiprismatic geometry and twisted square antiprismatic geometry (Fig. S10 - S13 in the supplementary materials). The Tb(III) and Gd(III) probes were prepared and purified using the same methodologies with the appropriate lanthanide triflate salt (see Fig. S8 and S14 in the supplementary materials for the  $^1\text{H}$  NMR spectra of the Tb(III) ion complexes). All complexes were analysed for purity using analytical HPLC, conducted on a phenyl analytical column with isocratic elution. For the PTE based lanthanide probes, **13**, **14**, **17**, **18** and **19** a single peak was observed (Fig. S17, S18 and S21 – S23 in the supplementary materials). The retention times of these peaks were significantly different to that of the starting materials (Fig. S15 – S16 in the supplementary materials), confirming the formation and isolation of a single pure compound in each case. Two peaks with similar retention times were observed in all the HPLC traces of the folic acid based lanthanide probes, **15**, **16** and **20** (Fig. S19, S20 and S24 in the supplementary materials) which were attributed to the formation of the two regio-isomers ( $\alpha$  and  $\gamma$ ). The area of the first peak was approximately twice the area of the second peak in all of the HPLC traces recorded, which is consistent with literature reports for the formation of the regio-isomers [45]; the  $\alpha$ -isomer is known to form at approximately half the rate of the  $\gamma$ -isomer due to the increased steric hindrance present at this carboxylic acid moiety. In line with common practice, the regio-isomers of the folic acid based probes were not separated into individual components [45-48]. The effect that the different isomers have on cell uptake in relation to probe structure is currently being investigated.

### 3.2. Lifetimes and $q$ values

The emission lifetimes of complexes **13-17** were determined to provide information for future time-gated measurements and cell imaging. The lifetimes also allow the  $q$  value (the number of metal bound waters) to be quantified for each probe, to confirm the coordination environment around the lanthanide ion. The inner sphere hydration state ( $q$ ) (i.e. the number of metal bound water molecules) was defined by measuring the excited state lifetimes (measured as tau ( $\tau$ ) values) of the Eu(III) and Tb(III) probes, **13-17**, in H<sub>2</sub>O and D<sub>2</sub>O, respectively. The  $q$  values were calculated using  $q = 1.11 (k_{\text{H}_2\text{O}} - k_{\text{D}_2\text{O}} - 0.31)$ [49] for Eu(III) probes and  $q = 4.2 (k_{\text{H}_2\text{O}} - k_{\text{D}_2\text{O}})$ [50] for Tb(III) probes (**Table 1**). The tau ( $\tau$ ) values found in **Table 1** are the reciprocal of  $k$  used in the two equations and were determined using the Cary Eclipse Win FLR lifetime program. A  $q \sim 1$  was found for all probes, indicating that each of the Eu(III) and Tb(III) probes possessed one metal bound water molecule, supporting the formation of an 8 coordination complex with the ligand. Due to the similar solution chemistry exhibited by the lanthanides it was reasonable to assume that the Gd(III) probes, **18-20**, also possessed one metal bound water. The presence of the metal bound water is important for Gd(III) complexes to be used as contrast agents for MRI applications. The relaxivity of these complexes could not be accurately determined due to issues associated with the long term stability of these probes in their solid state during transport; long term stability is associated with the coupling of folate/PTE to the linker and not the chelate. Elemental analysis results of the degraded products following transport supported this; results could only be fitted to Ln(III) chelate and not to Ln(III) chelate-folate/PTE conjugates. Degradation of the probes was also easily identifiable due to a change in colour of the solid. However it is important to note that all complexes retained sufficient aqueous stability for use in the analysis of photophysical properties and cell uptake studies. These studies were performed immediately following synthesis to minimise the potential for degradation. <sup>1</sup>H NMR and HPLC analysis of the probe solution following photophysical analysis confirmed that the probe structure was only affected during transport.

### 3.3 UV-Visible, fluorescence and lanthanide ion emission spectroscopy

After the synthesis, the probes photophysical properties were evaluated, including the UV-Visible, fluorescence and lanthanide ion emission responses of the probes over physiological

pH ranges. The photophysical studies were designed to provide information on the optimal excitation wavelength, the effect of pH on the probes and how the structure of the probes affects the photophysical properties. The UV-Visible absorption, fluorescence and lanthanide luminescence emission of the probes was measured at 298 K as a function of pH, in 100% aqueous solution [ $I = 0.01$  M (NaCl)] (see **Figure 2** for the UV-Visible absorption, fluorescence and Eu(III) emission spectra and a plot of the changes vs pH of **16** as an example (see supplementary materials Fig. S25-S28 for corresponding data for **13**, **14**, **15** and **17**)).

All of the folic acid and PTE based probes at pH 3 showed both an intense absorption band centred around 280 nm, which upon titration with base underwent a bathochromic shift to approximately 260 nm or less, and a small absorption band centred around 360 nm, which increased in molar absorptivity and underwent a hypsochromic shift upon titration with base [51]. A plot of the molar absorbance changes vs pH for **13**, **14**, **15**, **16** and **17** showed that the molar absorptivity was significantly altered between pH 6 – 8 and only slightly altered below pH 4. The molar absorptivity changes between pH 6 – 8 can be attributed to the protonation of N<sup>3</sup>H/CO of the pteridine ring in both targeting moieties;  $pK_a$  8.0 (N<sup>3</sup>H/CO) for both folic acid and pterioic acid. The shift of the  $pK_a$  to a lower value was assigned to the electron withdrawing effect of the Eu(III) complex [52]. The influence on molar absorptivity below pH 4 is unlikely to be replicated in a cellular environment and hence will not be discussed in detail here.

The molar absorbance changes as a function of pH were measured to inform the choice of appropriate excitation wavelength(s) for the fluorescence and Ln(III) emission spectroscopy. Excitation wavelengths are commonly chosen from absorption maxima(s). Furthermore, excitation wavelengths chosen for biological applications will ideally not cause cell damage (wavelengths below 280 nm are known to cause cell damage [53, 54]) and will match available confocal microscopy lasers (360 nm and 720 nm using two photon). However, the low molar absorbance of the probes at 360 nm may only result in low energy emissions and this might not be ideal for cellular imaging (low energy emissions are difficult to observe at concentrations required for cell studies) or to investigate any trends between structure and

emission properties. Therefore, both 280 nm and 360 nm wavelengths were chosen to monitor the fluorescence and Ln(III) emission from the probes as a function of pH. Both excitation wavelengths resulted in a large fluorescence emission band centred at ~ 450 nm. A plot of the fluorescence emission at 450 nm vs pH shows that the fluorescence is significantly modulated above pH 6. This is similar to the molar absorptivity and hence the change in fluorescence emission intensity was attributed to the protonation of N<sup>3</sup>H/CO of the pteridine ring in both targeting moieties. Below pH 4 the probes were shown to differ in the extent to which fluorescence emission was sensitive to pH changes. However as it is unlikely that the probes will encounter conditions as acidic as this in cells (cancer cells vary pH 5 – 8) [55] fluorescence change below pH 4 will not be discussed herein.

The most important photophysical response to be investigated against changes in pH is the Ln(III) emission response; it is expected that only the Ln(III) ion emission that will be detected using confocal microscopy. Characteristic Ln(III) emission bands were observed from the lanthanide ions when excited indirectly at either 280 nm or 360 nm for all the probes. The Tb(III) probes exhibited higher emission intensities compared to the Eu(III) probes. This is as expected as the excited states of Eu(III) are known to be more sensitive to quenching via -OH vibration deactivation pathways [56]. Therefore, Tb(III) ion probes may be more ideally suited to investigating molecules of interest or targeting receptors which are present in low concentration in cellular applications.

Interestingly, the type of targeting moiety was found to alter the Ln(III) emission response to pH; the Ln(III) emission from the folic acid based probes, **15** and **16**, was found to be relatively pH insensitive, whereas for the PTE based probes, **13**, **14** and **17**, some Ln(III) ion emission quenching under acidic conditions was observed. This is in contrast to both the molar absorbance and fluorescence emission where no difference in pH response was observed between targeting moiety.

The lack of pH sensitivity in the Eu(III) emission as a function of pH of the folic acid based probes, **15** and **16** can be attributed to the extra glutamic acid residue in folic acid which acts

to increase the distance between the aromatic moiety and the Eu(III) ion. This was consistent with the observation that the effective population of the Eu(III) ion via either the Dexter or Förster energy transfer mechanisms reduces as distance increases. Therefore, the effect from the protonation at the N<sup>3</sup>H/CO of the pteridine ring of folic acid is too far removed from the Eu(III) ion to affect the sensitisation process in the folic acid based probes. Therefore the emission from folic acid based probes will directly reflect the local probe concentration regardless of the pH variations that are known to occur within cancer tissues [55, 57].

A comparison of the PTE and folate based Eu(III) probes, **13**, **14**, **15** and **16**, showed that the length of the linker influenced the spectral properties of the probes. As the distance between the aromatic moiety and the Eu(III) ion increased, the emission from the Eu(III) decreased. This is further evidence that the Dexter or Förster energy transfer mechanisms reduces as distance increases.

### 3.4. Cellular uptake

The cellular uptake of Eu(III) probes was investigated using the human endothelial carcinoma cell line HeLa, which is known to express high amounts of the folate receptor [58]. Cells were incubated with the probes overnight, washed and lysed by HNO<sub>3</sub>. The intracellular concentrations of the probes were determined by the measurement of Eu(III) ion by ICP-MS (**Table 2**). The viability of the cells (as assessed by trypan blue exclusion) was not affected by incubation with the probes at the tested concentration. This indicates that the probes were not toxic to cells; an essential property for live cell imaging applications.

The folic acid based probes exhibited a higher intracellular concentration compared to the PTE based probes containing the same linker group (**15** > **13**, **16** > **14**). This indicates that the affinity of the receptor for PTE is reduced when compared with folic acid, and therefore the use of the synthetically simpler PTE is outweighed by the reduced uptake efficiency.

The ICP-MS cell uptake studies also showed that when a smaller distance between the targeting motif and the lanthanide chelate was employed that the percentage of probe internalised was increased. This is an interesting finding, when considered contextually in relation to the folate receptor targeting literature. The most commonly used linker structure for probe development includes long and structurally complicated linkers such as PEG, peptides and carbohydrates. The rationale behind the use of such long linkers is that research has shown that the size of the linker is associated with the flexibility of the probe; and reduced cell binding has been traditionally attributed to linkers with poor flexibility [59]. Hence, these larger linkers have been employed even though they significantly increase the synthetic difficulty of probe preparation and the overall molecular weight of a probe. These findings suggest that there is no need to employ such large and complicated linker structures, especially as increased molecular weight is often associated with macropinocytic uptake [60]. Therefore, the size of the linker group can be kept to a minimum for future applications.

#### 4. Conclusion

In conclusion, we have designed, synthesised and characterised a series of water-soluble folate receptor targeted lanthanide probes, which demonstrated cellular uptake in a HeLa cell line. All probes were found to have a  $q \sim 1$ , with eight binding sites for the core lanthanide ion. In addition, the probes were found to not perturb cell viability even at high concentrations. Compared to fluorescent probes targeted to the folate receptor, these new probes have the advantage of being easily adapted to enable the detection through MRI and time-gated luminescence methodologies for future *in vivo* applications.

We demonstrated that the targeting moiety was important for the efficacy of probe uptake: with folic acid based probes exhibiting more cellular uptake than the corresponding PTE based probes. Furthermore, the increased uptake was not associated with the increased flexibility of a longer linker; and thus a shorter linker was optimal for both cellular uptake and emission from the Eu(III) ion.

The folic acid based probes were pH insensitive and this makes them ideal for localisation in cancers where the pH is known to vary. The information gained in this work is currently being applied to the development of new lanthanide molecular probes with higher emission quantum yields, which will support live cell imaging and have the potential to provide new reagents for cancer detection and imaging.

#### **Acknowledgements:**

David Parker, University of Durham for advice on coupling marocycles to folic acid. A. Dean Sherry, Advanced Medical Imaging Center, Southwestern Medical Center, University of Texas at Dallas for relaxivity measurements. University of South Australia for funding this research.

#### **References**

- [1] K. Kiyose, H. Kojima, T. Nagano, *Chem. -Asian J.*, 3 (2008) 506-515.
- [2] L.D. Lavis, R.T. Raines, *Chem. Biol.*, 3 (2008) 142-155.
- [3] D.W. Domaille, E.L. Que, C.J. Chang, *Nat. Chem. Biol.*, 4 (2008) 168-175.
- [4] N.C. Shaner, P.A. Steinbach, R.Y. Tsien, *Nat. Methods*, 2 (2005) 905-909.
- [5] A.P. Alivisatos, W.W. Gu, C. Larabell, *Ann. Rev. Biomed. Eng.*, 7 (2005) 55-76.
- [6] N. Kaji, M. Tokeshi, Y. Baba, *Anal. Sci.*, 23 (2007) 21-24.
- [7] J.F. Weng, J.C. Ren, *Curr. Med. Chem.*, 13 (2006) 897-909.
- [8] K.L. Haas, K.J. Franz, *Chem. Rev.*, 109 (2009) 4921-4960.
- [9] S.U. Pandya, J. Yu, D. Parker, *Dalton Trans.*, (2006) 2757-2766.
- [10] S. Achilefu, *Tech. Cancer Res. Treat.*, 3 (2004) 393.
- [11] I. Johnson, *Histochem. J.*, 30 (1998) 123-140.

- [12] V. Ntziachristos, C. Bremer, R. Weissleder, *Eur. Radiol.*, 13 (2003) 195-208.
- [13] S.K. Deo, S. Daunert, *Anal. Biochem.*, 289 (2001) 52-59.
- [14] P. van Roessel, A.H. Brand, *Nat. Cell. Biol.*, 4 (2002) E15-E20.
- [15] H.C. Manning, T. Goebel, R.C. Thompson, R.R. Price, H. Lee, D.J. Bornhop, *Bioconjugate Chem.*, 15 (2004) 1488-1495.
- [16] A.P. Kozikowski, M. Kotoula, D. Ma, N. Boujrad, W. Tückmantel, V. Papadopoulos, J. *Med. Chem.*, 40 (1997) 2435-2439.
- [17] J. Sudimack, R. Lee, *Drug Delivery Rev.*, 41 (2000) 147-162.
- [18] A.R. Hilgenbrink, P.S. Low, *J. Pharm. Sci.*, 94 (2005) 2135-2146.
- [19] E. Sega, P. Low, *Cancer and Metastasis Rev.*, 27 (2008) 655-664.
- [20] I. Hemmilä, V. Laitala, *J. Fluoresc.*, 15 (2005) 529-542.
- [21] D.J. Bornhop, J.M.M. Griffin, T.S. Goebel, M.R. Sudduth, B. Bell, M. Motamedi, *Appl. Spectrosc.*, 57 (2003) 1216-1222.
- [22] D. Dosev, M. Nichkova, M. Liu, B. Guo, G. Liu, Y. Xia, B.D. Hammock, I.M. Kennedy, in: *Proc. SPIE*, 2005, pp. 473-481.
- [23] S. Laurent, L.V. Elst, R.N. Muller, *Contrast Media Mol. Imaging*, 1 (2006) 128-137.
- [24] S. Aime, M. Botta, E. Terreno, *Adv. Inorg. Chem.*, Volume 57 (2005) 173-237.
- [25] M.A. Kirchin, V.M. Runge, *Top. Magn. Reson. Imaging*, 14 (2003) 426-435.
- [26] M.-F. Bellin, *Eur. J. Radiol.*, 60 (2006) 314-323.
- [27] L. Armelao, S. Quici, F. Barigelletti, G. Accorsi, G. Bottaro, M. Cavazzini, E. Tondello, *Coord. Chem. Rev.*, (2009).
- [28] J. Leonard, T. Gunnlaugsson, *J. Fluoresc.*, 15 (2005) 585-595.
- [29] T. Gunnlaugsson, J.P. Leonard, *Chemical Communications*, (2005) 3114-3131.

- [30] A.-M. Fanning, in, University of Dublin Trinity College, 2006.
- [31] A. Quintana, E. Raczka, L. Piehler, I. Lee, A. Myc, I. Majoros, A. Patri, T. Thomas, J. Mulé, J. Baker, *Pharm. Res.*, 19 (2002) 1310-1316.
- [32] M. Salazar, M. Ratnam, *Cancer and Metastasis Rev.*, 26 (2007) 141-152.
- [33] W. Moon, Y. Lin, T. O'Loughlin, Y. Tang, D. Kim, R. Weissleder, C. Tung, *Bioconjugate Chem.*, 14 (2003) 539-545.
- [34] Y. Lu, P. Low, *Cancer Immunol., Immunother.*, 51 (2002) 153-162.
- [35] N. Kamaly, T. Kalber, M. Thanou, J.D. Bell, A.D. Miller, *Bioconjugate Chem.*, 20 (2009) 648-655.
- [36] S.D. Konda, S. Wang, M. Brechbiel, E.C. Wiener, *Invest. Radiol.*, 37 (2002) 199-204.
- [37] C. Müller, C. Dumas, U. Hoffmann, P.A. Schubiger, R. Schibli, *Journal of Organometallic Chemistry*, 689 (2004) 4712-4721.
- [38] C.-Y. Ke, C.J. Mathias, M.A. Green, *J. Am. Chem. Soc.*, 127 (2005) 7421-7426.
- [39] D.A. Moore, *Organic Syntheses*, 85 (2008).
- [40] A.P. Krapcho, C.S. Kuell, *Synth. Commun.*, 20 (1990) 2559-2564.
- [41] G.L. Stahl, R. Walter, C.W. Smith, *J. Org. Chem.*, 43 (1978) 2285-2286.
- [42] E.J. New, A. Congreve, D. Parker, *Chem. Sci.*, 1 (2010) 111-118.
- [43] J. Rudovský, P. Cígler, J. Kotek, P. Hermann, P. Vojtíšek, I. Lukeš, J.A. Peters, L. Vander Elst, R.N. Muller, *Chem. Eur. J.*, 11 (2005) 2373-2384.
- [44] G. Tircso, B.C. Webber, B.E. Kucera, V.G. Young, M. Woods, *Inorg. Chem.*, 50 (2011) 7966-7979.
- [45] R. Lee, P. Low, *Drug Target.*, 25 (2000) 69-76.
- [46] A. Bettio, M. Honer, C. Muller, M. Bruhlmeier, U. Muller, R. Schibli, V. Groehn, A. Schubiger, S. Ametamey, *J. Nucl. Med.*, 47 (2006) 1153.

- [47] B. Stella, S. Arpicco, M.T. Peracchia, D. Desmaële, J. Hoebcke, M. Renoir, J. D'Angelo, L. Cattel, P. Couvreur, *J. Pharm. Sci.*, 89 (2000) 1452-1464.
- [48] D. Dubé, M. Francis, J.-C. Leroux, F.M. Winnik, *Bioconjugate Chem.*, 13 (2002) 685-692.
- [49] R.M. Supkowski, W.D. Horrocks, *Inorganica Chimica Acta*, 340 (2002) 44-48.
- [50] W.D. Horrocks, D.R. Sudnick, *J. Am. Chem. Soc.*, 101 (1979) 334-340.
- [51] Y.Y. He, X.C. Wang, P.K. Jin, B. Zhao, X. Fan, *Spec. Acta A: Mol. Biomol. Spec.*, 72 (2009) 876-879.
- [52] S.E. Plush, N.A. Clear, J.P. Leonard, A.-M. Fanning, T. Gunlaugsson, *Dalton Transactions*, 39 (2010) 3644-3652.
- [53] J. Cadet, S. Mouret, J.L. Ravanat, T. Douki, *Photochemistry and Photobiology*, 88 (2012) 1048-1065.
- [54] R.P. Sinha, D.-P. Häder, *Photochemical and Photobiological Sciences*, 1 (2002) 225-236.
- [55] L.E. Gerweck, K. Seetharaman, *Cancer Research*, 56 (1996) 1194-1198.
- [56] S.I. Klink, *Synthesis and photophysics of light-converting lanthanide complexes*, Universiteit Twente, 2000.
- [57] L.E. Gerweck, S. Vijayappa, S. Kozin, *Mol. Cancer Ther.*, 5 (2006) 1275-1279.
- [58] S. Chattopadhyay, Y. Wang, R. Zhao, I.D. Goldman, *Clin. Cancer Res.*, 10 (2004) 7986-7993.
- [59] C. Leamon, J. Reddy, *Advanced drug delivery reviews*, 56 (2004) 1127-1141.
- [60] C.P. Montgomery, B.S. Murray, E.J. New, R. Pal, D. Parker, *Accounts of Chemical Research*, 42 (2009) 925-937.

**Table 1** Luminescence lifetimes ( $\tau$ ) and inner sphere hydration numbers ( $q$ ).

**Table 2** The intracellular concentration of each Eu(III) probe.

**Figure 1.** The structure of **a**) folic acid (with  $\alpha$  and  $\gamma$  carboxyls) and **b**) PTE.

**Figure 2.** The spectra of compound **16** ( $3.2 \times 10^{-5}$  M), changes upon incremental addition of base (NaOH) in the presence of 0.01 M NaCl **a**) The UV-Vis spectra. **b**) The Fluorescence spectra ( $\lambda_{\text{ex}} = 280$  nm). **c**) The Eu(III) emission spectra ( $\lambda_{\text{ex}} = 280$  nm). **d**) The normalised changes of **15** as a function of pH in the presence of 0.01 M NaCl. The UV-Vis absorbance changes in the 260 nm transition (squares). The fluorescence emission intensity changes at 450 nm transition ( $\lambda_{\text{ex}} = 280$  nm, triangles). The Eu(III) emission intensity changes at 615 nm ( $\lambda_{\text{ex}} = 280$  nm, circles).

**Scheme 1.** The synthesis of the probes.

ACCEPTED MANUSCRIPT

Complex	$\tau$ (H <sub>2</sub> O)/ms	$\tau$ (D <sub>2</sub> O)/ms	$q$ ( $\pm 0.5$ )
<b>13</b>	$0.591 \pm 0.0$	$2.098 \pm 0.0$	1.0
<b>14</b>	$0.500 \pm 0.0$	$2.875 \pm 0.1$	1.5
<b>15</b>	$0.678 \pm 0.1$	$3.143 \pm 0.1$	0.9
<b>16</b>	$0.581 \pm 0.0$	$2.598 \pm 0.1$	1.1
<b>17</b>	$1.788 \pm 0.1$	$2.665 \pm 0.6$	0.8

Probe

Intracellular concentration ( $\mu\text{M}$ )

---

**13**

5.2

---

**14**

4.9

---

**15**

8.4

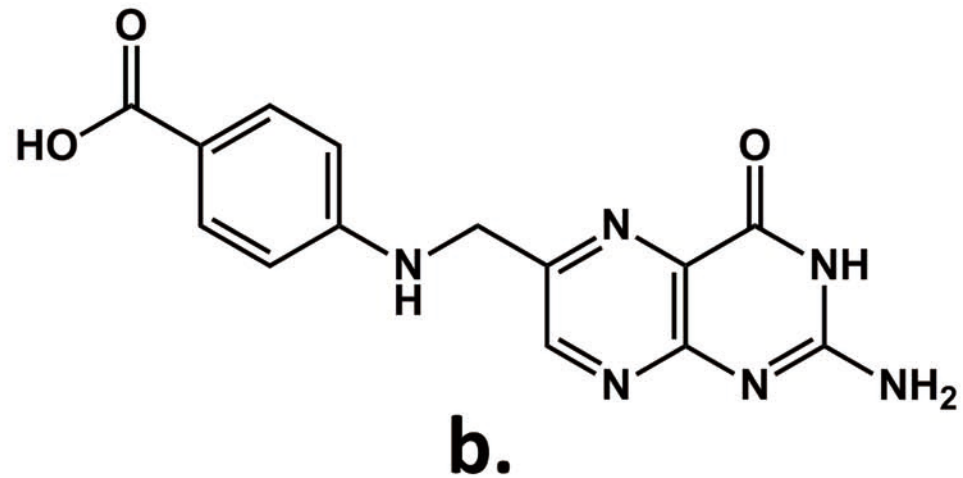
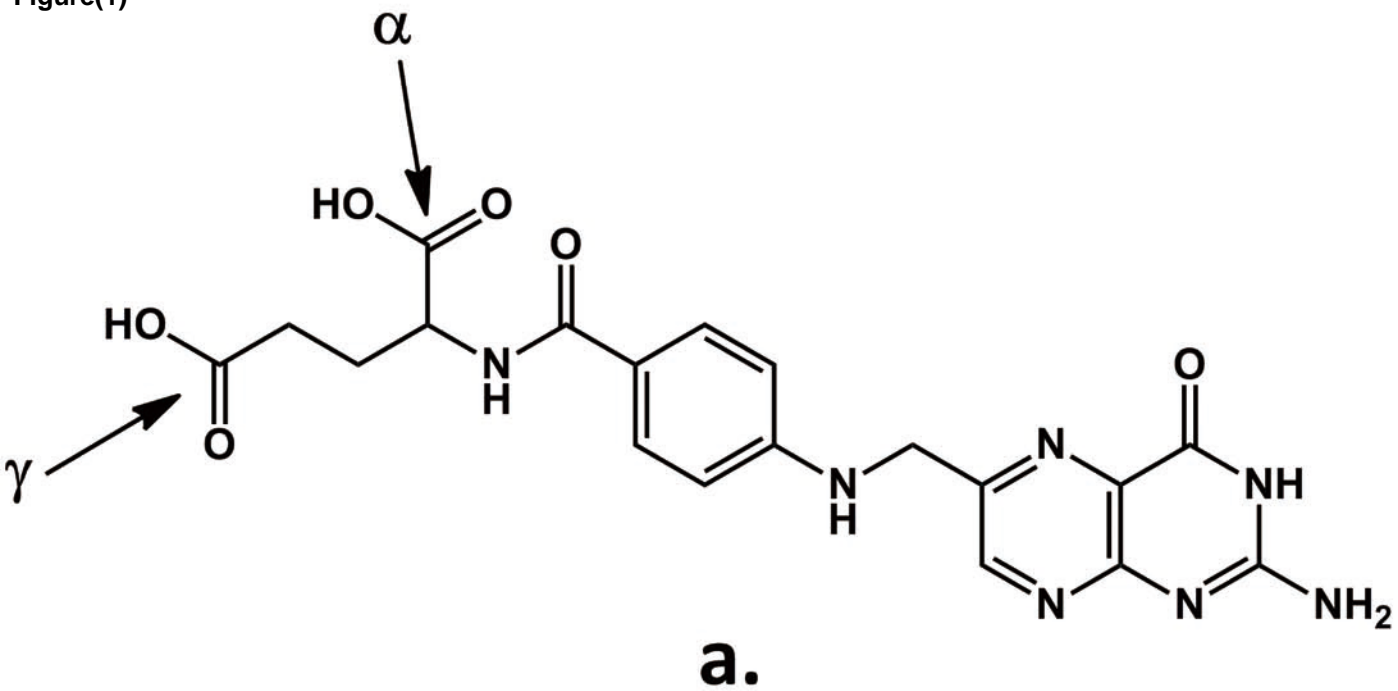
---

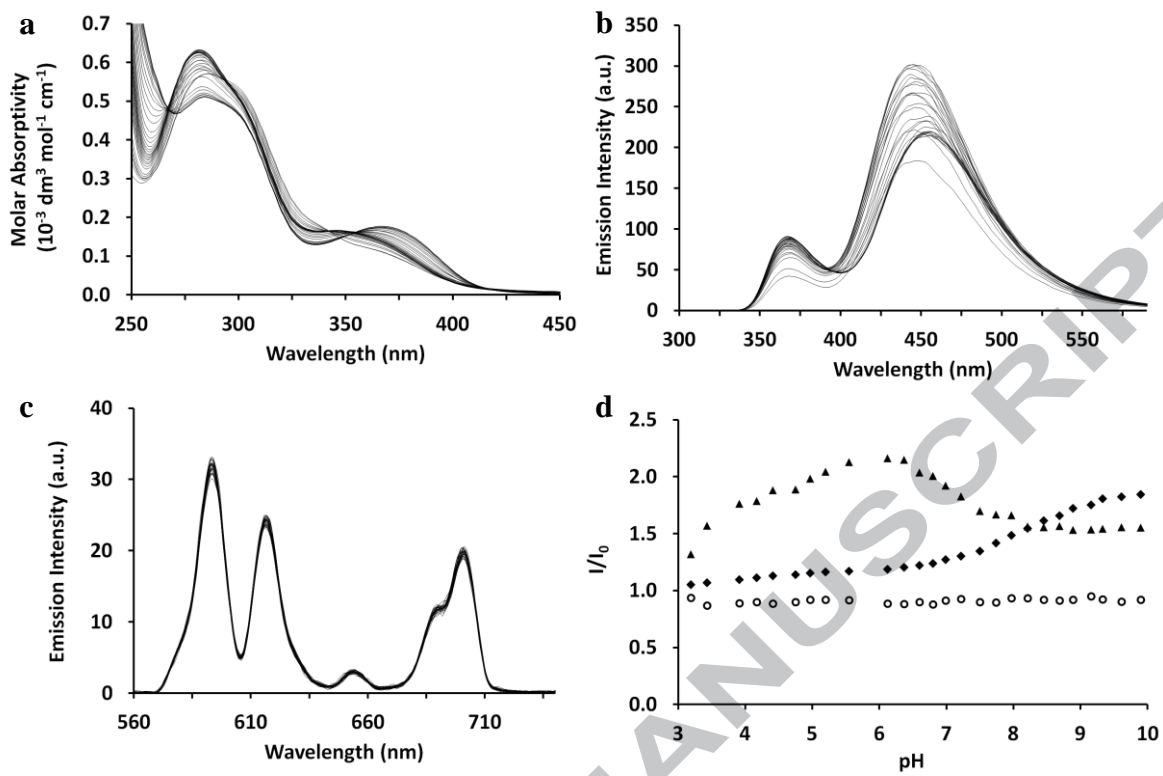
**16**

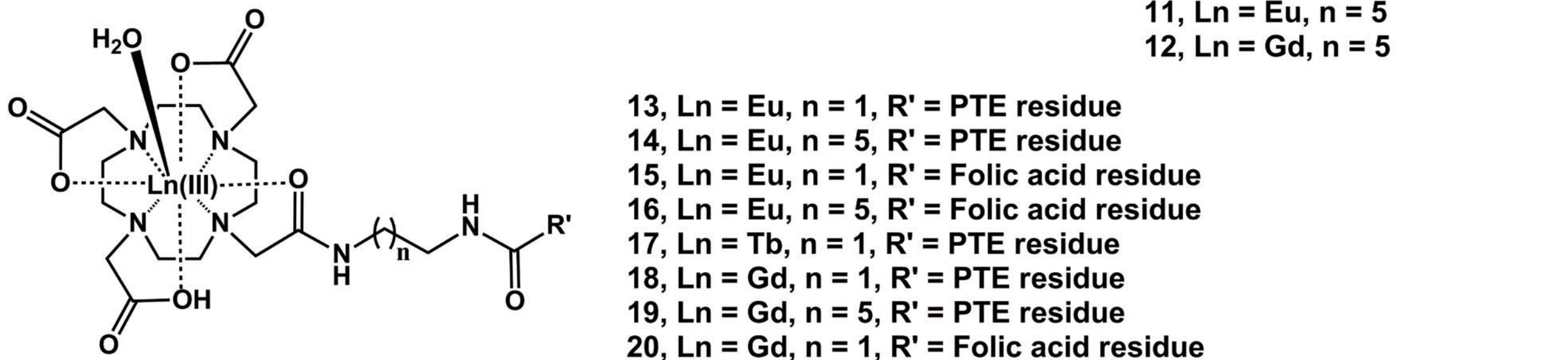
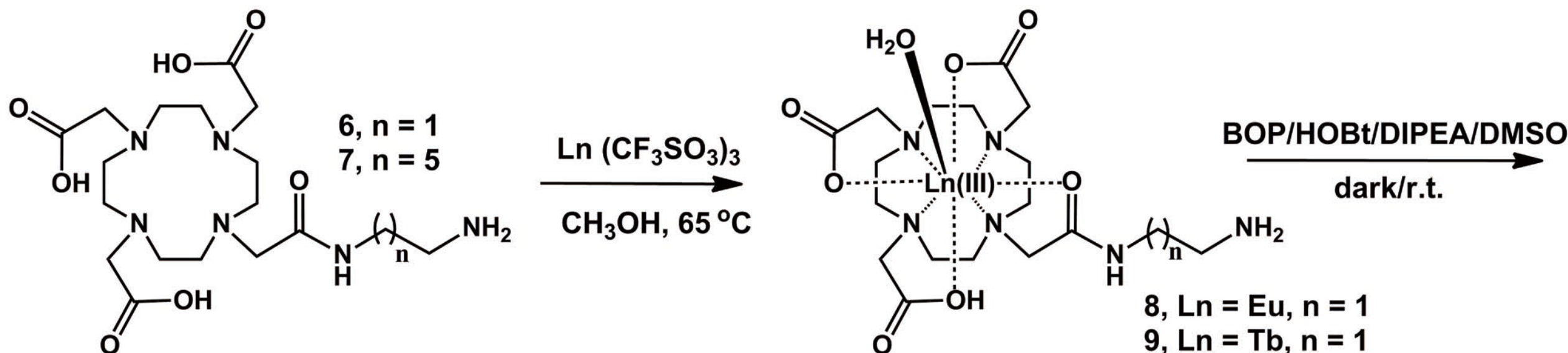
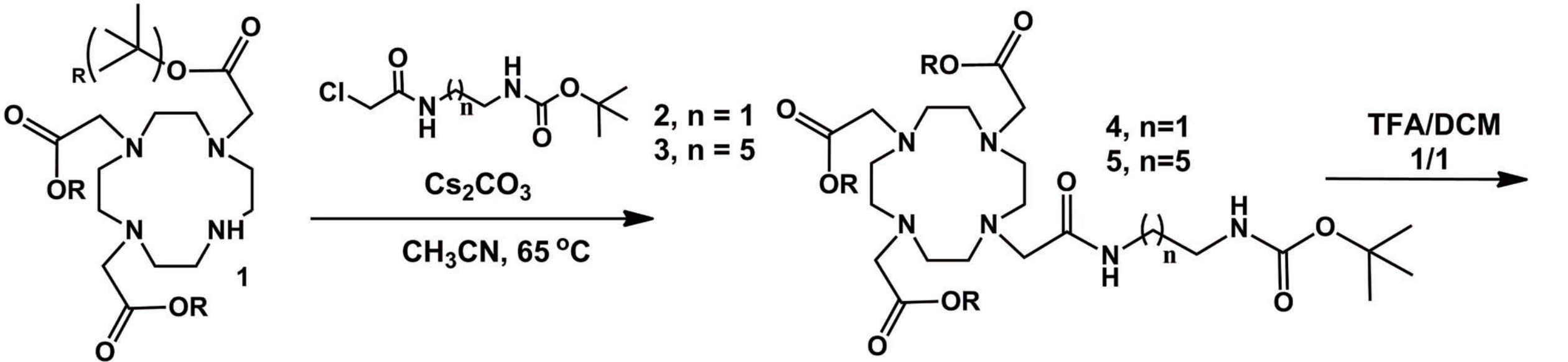
5.2

---

Figure(1)







- 8, Ln = Eu, n = 1  
 9, Ln = Tb, n = 1  
 10, Ln = Gd, n = 1  
 11, Ln = Eu, n = 5  
 12, Ln = Gd, n = 5

- 13, Ln = Eu, n = 1, R' = PTE residue  
 14, Ln = Eu, n = 5, R' = PTE residue  
 15, Ln = Eu, n = 1, R' = Folic acid residue  
 16, Ln = Eu, n = 5, R' = Folic acid residue  
 17, Ln = Tb, n = 1, R' = PTE residue  
 18, Ln = Gd, n = 1, R' = PTE residue  
 19, Ln = Gd, n = 5, R' = PTE residue  
 20, Ln = Gd, n = 1, R' = Folic acid residue

### Graphical abstract

A series of lanthanide(III) probes designed to target folate receptor were synthesised. The physical properties and cellular uptake of the probes were also investigated. The probe structure included a lanthanide(III) (Eu(III), Tb(III), Gd(III)) cyclen chelate which was linked to a targeting motif (folic acid or pteric acid) through a linker.

ACCEPTED MANUSCRIPT



### Highlights

- A series of water-soluble folate receptor targeted lanthanide probes have been designed and synthesised.
- The photophysical properties of the probes have been characterised.
- The cellular uptake of Eu(III) probes has been confirmed with HeLa cell line.

ACCEPTED MANUSCRIPT